J. Astrophys. Astr. (1983) **4**, 27–33

Intensity and Polarization Line Profiles in a Semi-Infinite Rayleigh-Scattering Planetary Atmosphere. II. Variations of Equivalent Width over the Disk

R. K. Bhatia and K. D. Abhyankar
Centre of Advanced Study in Astronomy, *Osmania University*, *Hyderabad 500007*

Received 1982 September 6; accepted 1983 January 3

Abstract. The study of the variation of equivalent width in a Rayleigh-scattering planetary atmosphere along the intensity equator and along the mirror meridian on which $\mu = \mu_0$ shows that the equivalent widths decrease monotonically towards the poles, the limb and the terminator with the following characteristics: (i) the weakest lines exhibit the maximum change; (ii) the I_r^e component shows more change than the I_l^e component; (iii) the decrease towards the limb or the terminator is not as sharp as that towards the poles; (iv) I_l^e component shows more decrease towards the limb while I_r^e component shows more decrease towards the terminator; and (v) the relation $W(\mu, \varphi; \mu_0, \varphi_0) = W(\mu_0, \varphi_0; \mu, \varphi)$ holds for the total intensity. These results are qualitatively in agreement with the observations of absorption bands in the spectra of Venus, Jupiter and Saturn.

Key words: Rayleigh scattering – line profiles – planetary atmospheres

1. Introduction

In a previous paper (Bhatia & Abhyankar 1982, hereafter called Paper I) we had discussed the variation of equivalent widths with phase angle in the integrated light of the planet, which represents an average over the disk. It would be useful to compute the variation of equivalent widths over the disk at different phase angles, because such a computation would provide additional information against which observations can be checked, although at present not many detailed studies have been made for Venus. Further, such computation for small phase angles can be applied to Jupiter and Saturn, whose range of phase angles is small.

Table 1. μ_0, μ and φ for points n the disk for $\alpha = 20$.

Position on disk†	Equator			Mirror meridian		
	μ_0	μ	φ	μ_0	μ	φ
0.1	0.94029	0.99999	0	0.00172	0.00172	2.7925
10	0.98481	0.98481	0	0.17101	0.17101	2.7872
20	...	...	...	0.33682	0.33682	2.7706
20.1	0.99999	0.93909	3.1416	...	...	...
30	0.98481	0.86602	3.1416	0.49240	0.49240	2.7399
40	0.93969	0.76604	3.1416	0.63302	0.63302	2.6891
50	0.86602	0.64279	3.1416	0.75441	0.75441	2.6061
60	0.76604	0.50000	3.1416	0.85287	0.85287	2.4635
70	0.64279	0.34021	3.1416	0.92542	0.92542	2.1896
80	0.50000	0.17365	3.1416	0.96985	0.96985	1.5555
85	0.42262	0.08715	3.1416	0.98106	0.98106	0.91813

† Longitude on intensity equator or co-latitude on mirror meridian. In the former case μ and μ_0 get interchanged for $\eta' = 20 - \eta$.

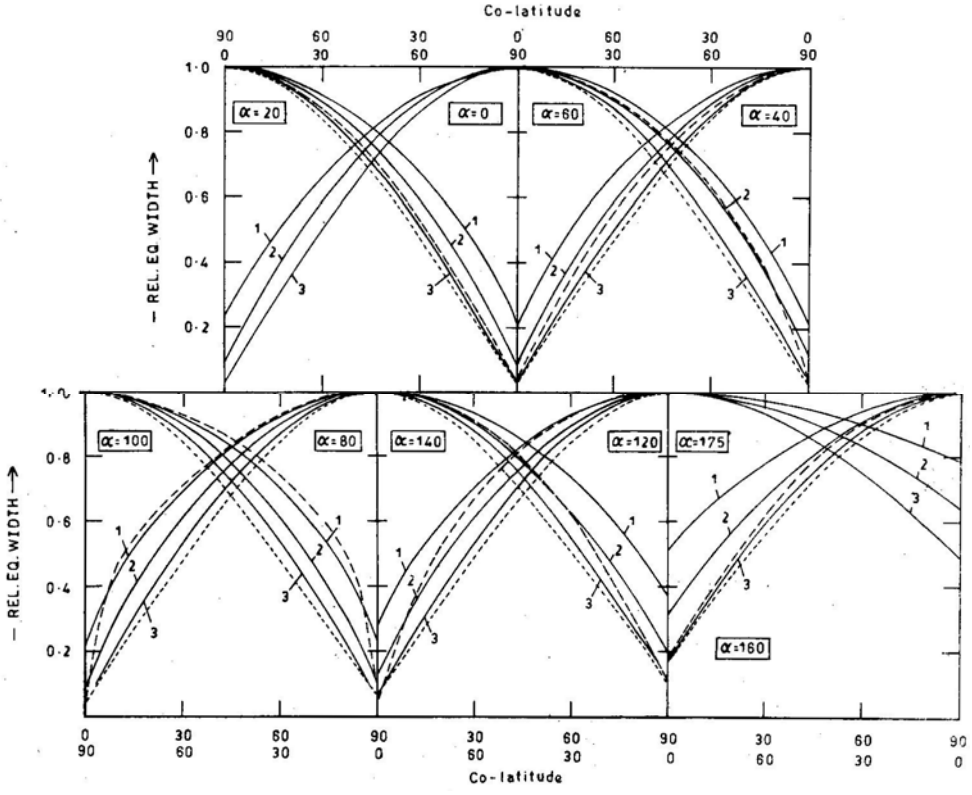

Figure 1. Variation of relative equivalent widths along the mirror meridian on which $\mu = \mu_0$ for total intensity for $\tilde{\omega} = 0.1$ (curve 1), $\tilde{\omega}_0 = 0.9$ (curve 2) and $\tilde{\omega}_0 = 0.9999$ (curve 3). Long and short dashed curves are for I_l^e and I_l^e components, respectively, for $\tilde{\omega}_0 = 0.9999$. The outer scale in abscissa refers to curves starting from upper left.

At the present juncture it is not necessary to compute the equivalent widths for a very detailed grid on the disk. Therefore, we have confined ourselves to computations along the intensity equator and along the meridian passing through the mirror point as defined by van de Hulst (1980). On this mirror meridian, $\mu = \mu_0$ and the longitude is equal to half the phase angle. Here, for each point of interest we use Equations (21), (22), (23) and (24) of Paper I for calculating μ, μ_0 and φ; they are given in Table 1 for α = 20. For points on the intensity equator $\varphi - \varphi_0 = 0$ or π according as the point lies within or outside the arc ES of Fig. 1 of Paper 1. Note that $\varphi - \varphi_0$ is not defined for either point E or S (Horak & Little 1965). Computation of the Stokes parameters along and perpendicular to the intensity equator requires the use of Equations (11), (12), (13), (29) and (30) of Paper I. These parameters were calculated at colatitudes 0.1, 10, 20, 30, 40, 50, 60, 70, 80 and 85 at phase angles 0, 20, 40, 60, 80, 100, 120, 140, 160 and 175. The Stokes parameters along with other auxiliary parameters are given by Bhatia (1982) for se lected colatitudes and phase angles. From the values of I_l^e and I_r^e, equivalent widths were calculated for three line strengths corresponding to ϖ_0 = 0.1, 0.9 and 0.9999 as outlined in Paper I. In all cases a continuum albedo of 0.997 was assumed. They are given in Table 2 for the mirror point and have been used for normalizing the equivalent widths at other points of the disk for the respective phase angles.

2. Variation of relative equivalent widths

2.1 *Variation along the Mirror Meridian*

By relative equivalent width we mean the ratio of equivalent width at a point on the

Table 2. Equivalent widths at the mirror point.

	α = 0	α = 20	α = 40	α = 60	α = 80
	.1949 + 2	.1993 + 2	.2124 + 2	.2320 + 2	.2452 + 2
I_l^e	.1765 + 1	.1814 + 1	.1961 + 1	.2175 + 1	.2311 + 1
	.3809 − 2	.3922 − 2	.4247 − 2	.4705 − 2	.4928 − 2
	.1949 + 2	.1932 + 2	.1881 + 2	.1796 + 2	.1676 + 2
I_r^e	.1765 + 1	.1745 + 1	.1687 + 1	.1590 + 2	.1452 + 1
	.3809 − 2	.3754 − 2	.3592 − 2	.3327 − 2	.2962 − 2
	.1949 + 2	.1962 + 2	.1992 + 2	.2010 + 2	.1961 + 2
I	.1765 + 1	.1779 + 1	.1812 + 1	.1828 + 1	.1767 + 1
	.3809 + 2	.3836 − 2	.3890 − 2	.3889 − 2	.3683 − 2
	α = 100	α = 120	α = 140	α = 160	α = 175
	.2267 + 2	.1758 + 2	.1237 + 2	.8352 + 1	.5515 + 1
I_l^e	.2087 + 1	.1516 + 1	.9369 + 0	.5220 + 0	.2660 + 0
	.4286 − 2	.2284 − 2	.1598 − 2	.7840 − 3	.2944 − 3
	.1519 + 2	.1322 + 2	.1081 + 2	.7884 + 1	.5257 + 1
I_r^e	.1275 + 1	.1057 + 1	.7976 + 0	.4992 + 0	.2543 + 0
	.2510 − 2	.1981 − 2	.1390 − 2	.7943 − 2	.2973 − 3
	.1788 + 2	.1496 + 2	.1154 + 2	.8126 + 1	.5391 + 1
I	.1567 + 1	.1240 + 1	.8428 + 1	.5110 + 0	.2604 + 0
	.3148 − 2	.2342 − 2	.1452 − 2	.7559 − 3	.2958 − 3

Note: First line for ϖ_0 = 0.1, second line for ϖ_0 = 0.9 and third for ϖ_0 = 0.9999. Last figure indicates power of ten.

disk to that at the mirror point. This variation for the total intensity along the mirror meridian for different phase angles is shown in Fig. 1 for the three line strengths corresponding to $\tilde{\omega}_0 = 0.1, 0.9$ and 0.9999. In addition, the variation for the Stokes parameter I_l^e (long dashes) and I_r^e (short dashes) are also shown for $\tilde{\omega}_0 = 0.9999$, the variation being similar for other albedos. An inspection of the figure shows that the equivalent widths decrease monotonically towards the poles by a significant amount, the decrease being a function of the line strength, with the weakest line showing the maximum change. This dependence on line strength is akin to what we have already seen in Paper I for the variation of the relative equivalent widths with phase angle in the integrated light; there also the weakest line showed the maximum change. An explanation of this phenomenon on the basis of effective depth of line formation will be given else where. Furthermore, the rate of decrease of relative equivalent widths with colatitude increases slightly till phase angle 60, after which there is a continuous decrease.

The relative equivalent width curves for the Stokes component I_r^e show a smooth change with colatitude at all phase angles, the change being more than that for either the Stokes component I_l^e or the total intensity I. At all the phase angles the change for the I_l^e component is the least sharp near the equator. However, while at extreme phase angles the change is smooth at all colatitudes, for the intermediate phase angles ($40 < \alpha < 140$), there is a sharp decrease at low colatitudes. This occurs because of a steep drop in the value of the I_l^e component for higher albedos. For example, between colatitudes 30 and 20, the continuum intensity for the I_l^e component drops by a factor of 1.5. The change at higher colatitudes is not so much. This change is high only for the I_l^e component because a look at the scattering diagram shows that the rate of change of the I_l^e component is maximum at $\alpha = 90$, there being a decrease at larger and smaller phase angles.

2.2 *Variation along the Equator*

Variation of equivalent widths along the intensity equator are shown in Fig. 2 for phase

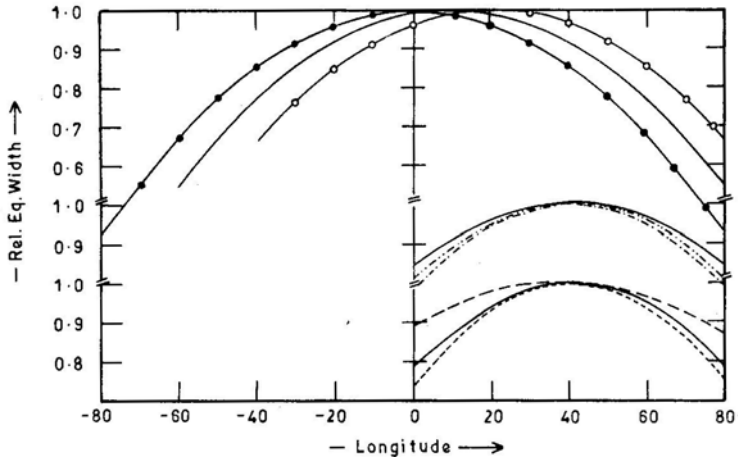

Figure 2. Variation of relative equivalent widths along the intensity equator. Among the upper curves, the curve with filled circles is for $\alpha = 0$, the plain curve is for $\alpha = 20$ and the curve with open circles is for $\alpha = 40$. Below this set are curves for $\alpha = 80$ for $\tilde{\omega}_0 = 0.1$ (solid), $\tilde{\omega}_0 = 0.9$ (dash and two dots) and $\tilde{\omega}_0 = 0.9999$ (dash and dot).The lowermost set is for $\alpha = 80$ for $\tilde{\omega}_0 = 0.9999$ for the total intensity I (solid), I_l^e (long dashes) and I_r^e (short dashes).

angles 0, 20, 40 and 80 for $\varpi_0 = 0.1$. In addition, for $\alpha = 80$ the curves for $\varpi_0 = 0.9$ and 0.9999 are also shown for the total intensity I and for $\varpi_0 = 0.9999$ alone for the Stokes components I_l^e (long dashes) and I_r^e (short dashes). All the equivalent widths are expressed in terms of the equivalent width at the mirror point.

These variations show some features which have already been noted in Section 2.1 for the variation along the central meridian: (1) the equivalent widths drop towards the limb and also towards the terminator; (2) this drop is an inverse function of the line strength; and (3) the equivalent widths for the I_l^e component do not show as much change as those for the total intensity I or the Stokes parameter I_r^e, the latter showing the maximum change.

In addition, the following features are different:

(i) The change in equivalent widths is not as sharp as that along the mirror meridian: this is because of the geometry. Along the mirror meridian both μ and μ_0 fall simultaneously while for the variation along the equator either μ or μ_0 becomes small (*cf.* Table 1).

(ii) There is a symmetry in the values of the equivalent widths for the total intensity about an angle equal to, half the value of the phase angle; this happens because about this angle, the values of μ and μ_0 are interchanged for equidistant longitudes [*cf.* Equations (21) and (22) of Paper I]. A consideration of Equations (11) and (12) of Paper I shows that the ratio I_v/I_c is the same when μ and μ_0 are interchanged, leading to the same values of the equivalent widths. This holds for the isotropic and anisotropic phase functions also (*cf.* Chandrasekhar 1960, p. 140), but not for the Stokes components I_l^e and I_r^e separately. We have thus the following relation for equivalent widths for the total intensity:

$$W(\mu, \varphi; \mu_0, \varphi_0) = W(\mu_0, \varphi_0; \mu, \varphi), \tag{1}$$

which is an obvious consequence of the general reciprocity principle.

(iii) Although there is a symmetry about the longitude defining the mirror meridian for the total intensity I for all phase angles, there exists an asymmetry in the variation for the Stokes components as noted in (ii) above. While the I_l^e component shows more decrease towards the limb, the drop for the I_r^e component is greater towards the terminator.

(iv) The rate of fall of equivalent widths decreases continuously with increasing phase angle.

2.3 *Variation of Relative Line Depth*

The variation of line depth defined by $(1 - z_v/z_c)$, ($z = I_l^e, I_r^e, I$), is also a measure of line strength like the equivalent width. Its variations along the equator is shown at the left of Fig. 3 and along the mirror meridian at the right of the same figure. For the former, the variation shown is for phase angle 0 for the total intensity for two albedos of 0.1 and 0.9, while for the latter the variation shown is for phase angle 80, for the same two albedos. In addition, the variation along the mirror meridian is shown for the I_l^e component (long dashes) and the I_r^e component (short dashes). It can be seen that the variation for $\varpi_0 = 0.1$ is not as large as that for $\varpi_0 = 0.9$, although for both the albedos the variation is similar to that of the relative equivalent widths. Very often one comes across observa-

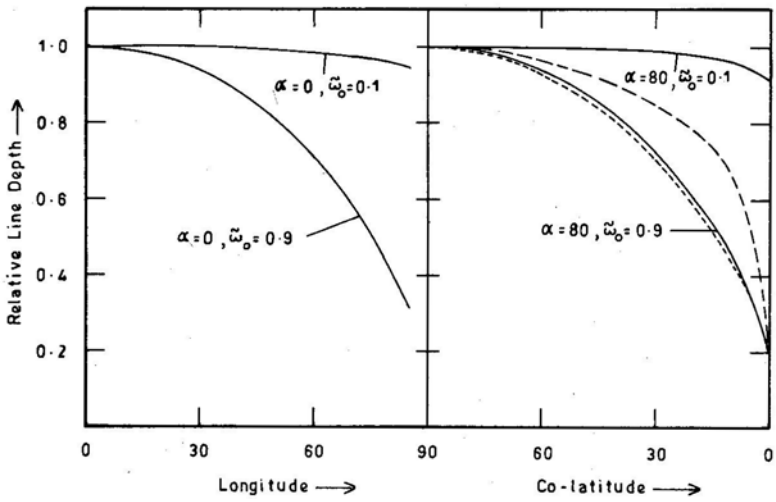

Figure 3. Relative line depths curves at left are for points along the equator and at right for points along the meridian on which $\mu = \mu_0$. The long dashed curve on the right refers to I_l^e component and the short dashed curve to I_r^e component for $\tilde{\omega} = 0.9$, $\alpha = 80$.

tions of the variation of line depths, especially for Jupiter. From the above it becomes clear that the variation for the line depths is of a different magnitude although the trend is the same. Therefore it would not be safe to club together the observations of equivalent widths and line depths.

Although we have used an extremely schematic model our results are qualitatively in agreement with observations as discussed below.

3. Comparison with observations

For Venus, there does not exist a homogeneous set of data for the variation of equivalent widths across the disk, an observational task made difficult by the day-to-day variations. However, observations of Young, Woszczyk & Young (1974) at phase angle $\alpha \sim 75$ indicate that the absorption is more towards the terminator than towards the limb. But the data are not sufficient to derive any definite conclusions. Evidently more observations are needed at different phase angles.

For Jupiter again the data are a little uncertain. Teifel (1976) summarizes the available observational data and concludes: (i) 'In the equatorial band of Jupiter, molecular absorption decreases by 10 to 20 per cent' as we go towards the limb (this is what is seen from Figs 2 and 3); and (ii) 'To the north and south of the equator, absorption in weak bands decreases with latitude; in medium and strong bands absorption increases in the latitude range 40-60, but not more than 5 to 7 per cent, sharply decreasing close to the poles'. Again, from Figs 1,2 and 3 these trends can be seen; since we are dealing with a homogeneous model, we cannot account for the increase in absorption for strong bands at mid-latitudes.

For Saturn, observations of Smith, McCord & Macy (1981) for the 6190 Å CH_4 band indicated a drop in equivalent widths both along the equator and along the cen-

tral meridian; they found that a homogeneous scattering model gave a good fit; a two layer and a reflecting-layer model did not fit the observations well. Figs 1, 2 and 3 show similar trends in agreement with observations.

Acknowledgements

We are thankful to Professor H. C. van de Hulst for his critical comments as a referee. RKB would like to thank the University Grants Commission, New Delhi, for the award of a fellowship.

References

Bhatia, R. K. 1982, *PhD Thesis*, Osmania University, Hyderabad.
Bhatia, R. K., Abhyankar, K. D. 1982, J. *Astrophys. Astr.*, **3**, 303 (Paper I).
Chandrasekhar, S. 1960, *Radiative Transfer*, Dover, New York.
Horak, H. G., Little, S. J. 1965 *Astrophys. J. Suppl. Ser.*, **11**, 373.
Smith, W. H., McCord, T. B., Macy, W. 1981, *Icarus*, **46**, 256.
Teifel, V. G. 1976, in *Jupiter*, Ed. T. Gehreis, University of Arizona Press, Tucson, p. 441.
van de Hulst, H. C. 1980, *Multiple Light Scattering*, Academic Press, New York.
Young, A. T., Woszczyk, A., Young, L. G. 1974, *Acta astr.*, **24**, 55.